New Insights into the Effects of Primary Hyperparathyroidism on the Cortical and Trabecular Compartments of Bone

Short title: Primary Hyperparathyroidism and Bone Microarchitecture

Thuy D.T. Vu[1]
Xiao Fang Wang[1]
Qingju Wang[1]
Natalie E. Cusano[2]
Dinaz Irani[2]
Barbara C. Silva[2]
Ali Ghasem-Zadeh[1]
Julia Udesky[2]
Megan E. Romano[2]
Roger Zebaze[1]
George Jerums[1]
Stephanie Boutroy[2]
John P. Bilezikian[2]
Ego Seeman[1]

[1]Department of Medicine and Endocrinology, Austin Health, University of Melbourne, Heidelberg, Australia;
[2]Department of Medicine and Division of Endocrinology, Metabolic Bone Diseases Unit, College of Physicians and Surgeons, Columbia University, New York, USA.

All authors contributed substantially to this work

Correspondence:
T.D.T Vu
Department of Endocrinology, level 2, Centaur Building, Austin Health
300 Waterdale Road Heidelberg West, Victoria 3081, Australia
Phone: +61394965489 Fax: +61394963365 Email: t.vu12@pgrad.unimelb.edu.au

Disclosures: R Zebaze, A Ghasem-Zadeh and E Seeman are inventors of the StrAx1.0 software. There is no other information to disclose.

Abstract

In primary hyperparathyroidism (PHPT), protracted elevation of serum parathyroid hormone (PTH) is held to be associated with cortical, but not trabecular, bone loss. However, an alternative explanation for the apparent preservation of trabecular bone is fragmentation of the cortex by intracortical remodeling. The cortical fragments resemble trabeculae and so may be erroneously included in the quantification of 'trabecular' bone density.

To test this hypothesis, we compared bone microarchitecture in 43 patients with untreated PHPT (mean 62.9 years, range 31-84) with 47 healthy age-matched controls and 25 patients with surgically treated PHPT (63.6 years, 30-82). Images of the distal radius and tibia were acquired using high-resolution peripheral quantitative CT and analysed using StrAx1.0, a new software program that quantifies bone morphology *in-vivo*. Results were expressed as the mean number of standardized deviations (SD) from the age-specific mean (Z scores, mean ± SEM).

In subjects with PHPT, total tibial cortical area was reduced -0.26 ± 0.08 SD; p=0.002). Cortical volumetric bone mineral density (vBMD) was reduced (-0.29 ± 0.06 SD; p<0.001) due to higher cortical porosity (0.32 ± 0.06 SD; p<0.001) and lower tissue mineralization density (-0.21 ± 0.06 SD; p=0.002). Medullary area was increased (0.26 ± 0.08 SD; p=0.002) and trabecular vBMD was reduced (-0.14 ± 0.04 SD; p<0.001).

In subjects who underwent successful parathyroidectomy, cortical area (-0.18 ± 0.10 SD; NS) and medullary area (0.18 ± 0.10 SD; NS) did not differ from controls. Cortical vBMD was reduced (-0.15 ± 0.05 SD; p=0.003) due to high porosity (0.15 ± 0.05 SD; p=0.006), values numerically lower than in untreated PHPT. Tissue mineralization density (-0.26 ± 0.04 SD;

p<0.001) and trabecular vBMD were reduced (-0.16 ± 0.04 SD, p<0.001). The results were similar in the distal radius.

In PHPT, chronically elevated endogenous PTH does not spare trabecular bone; it causes bone loss and microarchitectural deterioration in both cortical and trabecular compartments of bone.

Key words: bone microarchitecture, cortical porosity, high-resolution peripheral quantitative computed tomography, parathyroid hormone excess, tissue mineralization density

1.0 Introduction

Bone remodeling is surface dependent; it is initiated upon the three (intracortical, endocortical and trabecular) components of a bone's inner (endosteal) envelope. During young adulthood remodeling is balanced; the volume of old or damaged bone matrix excavated beneath the surface is replaced with an equal volume of new bone matrix[1]. During advancing age, remodeling becomes unbalanced; less bone is deposited than was removed so that each time a remodeling event occurs, focal structural deterioration ensues[2].

After menopause and in diseases such as primary hyperparathyroidism (PHPT), structural deterioration accelerates because the surface extent of remodeling increases and the negative bone multi-cellular unit (BMU) balance worsens[3].Remodeling upon trabecular surfaces thins and removes them.Remodeling upon endocortical surfaces thins the cortex and enlarges the medullary cavity. Intracorticalremodelingofthe cortex adjacent to the medullary canal cavitates it;Haversian canals coalesce worsening the porosity, thinning the cortex from 'within' and producing cortical remnants that look like trabeculae ('trabecularization')[4]. Intracortical remodeling and porosity account for 70% of total bone lost with age[4].

Parathyroid hormone (PTH) excess in PHPT produces cortical bone loss but is purported to preserve bone at trabecular sites[3-10]. This notion is based on finding normal or increased so-called 'trabecular' bone volumetric bone mineral density (vBMD) when assessed by noninvasive imaging and normal volume/total volume (BV/TV) using histomorphometry[3-10].

These disparate findings in the cortical and trabecular compartments are unusual because the three (endocortical, trabecular and intracortical) components of the endosteal (inner) envelope are contiguous; they are connected forming one inner surfaceof the mineralized bone matrix

volume; remodeling with loss of bone due to the negative bone balance is generally similar on each of these three components[11].

Thus, an alternative interpretation is that the normal or increased trabecular vBMD in PHPT is an artifact produced by inclusion of cortical remnants because they resemble true trabeculae, namely those of growth plate origin[4]. Cortical remnants are unlikely to confer normal bone strength because 'trabecularized' bone is chaotic and lacks the cancellous architectural design of trabecular bone[4].This view would also reconcile the increased vertebral fracture risk in PHPT, an anomaly if endogenous PTH preserved or increased trabecular bone volume in PHPT[6].

We hypothesized that (i) endogenous PTH in PHPT produces both cortical and trabecular bone loss, (ii) cortical remnants, which resemble trabeculae, are erroneouly included in the analysis of trabecular density, and (iii) there are residual deficits in both cortical and trabecular bone following successful parathyroidectomy. To test these hypotheses, we analyzed images of the distal radius and tibia acquired by high-resolution peripheral quantitative CT (HRpQCT), using StrAx1.0, a new software program that quantifies bone morphology *in-vivo*.

2.0 Materials and Methods

2.1 Patient cohort

Patients with untreated and surgically treated PHPT were recruited from Austin Hospital (Melbourne, Australia) and Columbia University Medical Center (New York, USA). We studied 43 untreated PHPT, 25 treated PHPT, and 47 age-matched healthy controls**(table 1)**. The healthy participants, previously published were recruited from the community[4]. The mean duration post-parathyroidectomy was 5.3 ± 5.3 years. The study was approved by the

Human Research Ethics Committee of Austin Health and the Institutional Review Board of Columbia University Medical Center. All subjects gave written, informed consent.

2.2 Image acquisition & analysis

Images of the non-dominant distal radius and tibia were acquired using high-resolution peripheral quantitative CT (HR-pQCT, XtremeCT, Scanco Medical AG, Brüttisellen, Switzerland) which has an isotropic voxel size of 82μm [12]. Daily quality control was carried out by scanning a phantom containing rods of hydroxyapatite (QRM Moehrendorf, Germany). Radiation exposure was ~3 μSv per measurement. Images were retrieved and analysed using a new software (StrAx1.0, StrAxCorp, Melbourne, Australia) [13]. Analysis was restricted to the 40 most proximal of the 110 slices in the region of interest as they have thicker cortices allowing accurate assessment of porosity.Results for bone compartments, cortical morphology and trabecular vBMD were derived from StrAx1.0 analysis. Trabecular morphology (i.e., trabecular number, thickness and separation) was derived from Scanco Medical AG software analysis.

Using curve profile analysis, bone is segmented from the soft tissue background and then into its compact-appearing cortex, outer and inner transitional zone, and medullary (trabecular) compartment. Once deposited, matrix rapidly undergoes primary mineralized reaching ~80% of its peak mineralization density within days to weeks. StrAx1.0 excludes voxels with attenuation between 80-100% of the maximum attenuation produced by 1200mghydroxyapatite(HA)/cc, fully mineralized bone, when quantifying porosity, because these voxels contain younger bone at various stages of secondary mineralization responsible for the heterogeneity in mineralization that could be mistakenly interpreted as porosity. These voxels are unlikely to contain Haversian canals (pores in cross section) because few are less than 25 microns diameter).Porosity is quantified by estimating the void fraction of

each of the remaining voxels. To do so, the mineralized bone matrix volume of each voxel is quantified using an interpolation function derived from two referents;(i) the attenuation of voxels containing fully mineralized bone matrix (equivalent to thatproduced by1200mgHA/cc)are assigned a value of 100% and (ii) voxels that are empty with an attenuation equivalent to background are assigned a value of 0%. The volume fraction of a voxel that is void (otherwise known asporosity) is 100% minus the mineralized bone matrix fraction. The porosity of the compartment is the average void volume fraction of all composite voxels which vary in their proportions of void and mineralized bone matrix, not only the completely empty voxels [13].

To quantify tissue mineralization density, only voxels with attenuation values between 80 and 100% of the attenuation producedby 1200mgHA/cc are used. The difference between the attenuation produced by voxels containing only mineralized bone and the attenuation produced by background represents the attenuation produced by the mineral within the bone matrix. Tissue mineral density is the ratio of the attenuation produced by the mineral in the bone matrix to the attenuation produced by 1200 mgHA/cc.Frequency distribution curves depicting the composition of the cortex according to voxel content (empty, mineralized bone matrix only, varying proportions of each) were also computed [13].

Segmentation and quantification of porosity is accurate with r^2 ranging from 0.88 to 0.99 at the distal radius and tibia which assessed bone morphology *in-vivo* compared to gold standard micro-CT (19 μm voxel size). Reproducibility, the root mean square error of the coefficient of variation is 0.5 to 3.0%.

Total cortical area, the compact-appearing cortical area, OTZ and ITZ and medullary area were expressed as a percentage of the total CSA to adjust for bone size. Tissue mineralization density was determined by the attenuation produced by voxels whose volume was occupied by bone matrix and no void volume.

2.3 Biochemical analyses

Serum intact PTH and 25(OH) vitamin D were measured using an electro-chemiluminescence immunoassay (Roche Modular E170, Switzerland). Serum calcium and phosphate were analysed by automated techniques (unicel DXC 800, Beckman Coulter Inc, USA).

2.4 Statistical analyses

Measurements were expressed as mean Z scores (± SEM), the number of standardised deviations (SD) from age-, sex- height- and weight- adjusted mean of zero based on the linear regression in 47 healthy controls. T-tests assessed whether the Z scores differed from zero. Group comparisons were made using ANOVA. The contribution of cortical porosity and tissue mineralization density to the variance in cortical vBMD was determined using stepwise regression analysis. A frequency distribution curve of mineralized bone matrix content of compact-appearing cortex was plotted for the three groups. A p value of <0.05 was considered to be statistically significant. Analyses were conducted using SPSS version 20 software (SPSS Inc, Chicago, USA).

3.0 Results

3.1 Untreated PHPT vs. controls

As shown in **Figure 2** and **Table 2**, for the distal tibia, relative to controls, untreated patients with PHPT had reduced total cortical area (compact-appearing plus transitional zone) (-0.26 ± 0.08 SD, p = 0.002) and increased medullary area (0.26 ± 0.08 SD, p = 0.002). The compact-

appearing cortical area and outer transitional zone area were each reduced (-0.31 ± 0.08 SD, p <0.001 and -0.43 ± 0.15 SD, p = 0.007 respectively). The inner transitional zone area was not reduced.

Total cortical vBMD was reduced (-0.29 ± 0.06 SD, p <0.001) due to (i)increased cortical porosity in the compact-appearing (0.13 ± 0.04 SD, p=0.003) and in the transitional zones (OTZ, 0.16 ± 0.05 SD, p = 0.002 and ITZ, 0.32 ± 0.04 SD, p<0.001) and (ii) reduced tissue mineralization density (-0.21 ± 0.06 SD, p = 0.002) of the surrounding bone matrix.Of the reduction in cortical vBMD, 97.5% was attributable to the increased cortical porosity with only2.0% attributable to lower tissue mineralization density. Cortical vBMD and cortical porosity correlated inversely with r^2= 0.975 before, and 0.983 after,adjustment for tissue mineralization (both p <0.001). The void bone matrix mineralization distribution curve was shifted left relative to controls (**Figure 4**). Trabecular vBMD was reduced (-0.14 ± 0.04 SD, p <0.001) relative to controls. Trabecular separation was increased (0.07 ± 0.03 SD, p = 0.030) but trabecular number (-0.06 ± 0.05 SD; p=0.250) and the trabecular thickness (0.10 ± 0.06 SD; p=0.110) did not differ from controls (**Figure 3**).

3.2 Treated PHPT vs. controls

In successfully surgically treated patients, relative to controls, total cortical area was not reduced and medullary area was not increased. The compact-appearing cortical areawasreduced (-0.22 ± 0.09 SD; p=0.03). The outer and inner transition zone areas were no different to controls. Total cortical vBMD was reduced (-0.15 ± 0.05 SD; p=0.003). Overall, total cortical porosity was increased due to increased ITZ porosity; porosity in compact-appearing cortex and OTZ were no different to controls. Tissue mineralization density distribution was shifted to the left relative to controls. Trabecular vBMD was reducedrelative to controls (-0.16 ± 0.04 SD; p <0.001) due to reduced trabecular number (-0.19 ±0.05 SD;

p<0.001) not thickness (0.09 ± 0.08 SD; NS). Trabecular separation was increased (0.24 ± 0.09 SD; p<0.010) (**Figure 3**).

3.3 Treated PHPT vs. untreated PHPT

In successfully surgically treated patients, total cortical area, compact-appearing cortical area and outer transitional zone areawere 3, 10, and 15%larger thanin untreated patients respectively; none reaching significance. The inner transition zone area was no different. Cortical vBMD was 8% greater than in the untreated patients (p = 0.075). Total cortical porosity, compact-appearing cortex, outer and inner transitional zone porositywerehigherrelative to controls,but 9, 22, 16, and 2%less than in the untreated patients with none reaching significance. Tissue mineralization density was lowrelative to controls,but no differentwhen compared tothe untreated group (p=NS) (**Figure 2and Table 2**). Trabecular vBMD, number, thickness and separation were no different to the untreated patients. Results for the distal radius were attenuated but showed a similar trend to that of the distal tibia.

4.0 Discussion

We report that endogenous PTH excess as seen in PHPT is deleterious to both cortical and trabecular bone in the distal tibia. Specifically, (i) mean cortical bone area was reduced due to remodeling upon the intracortical surface eroding the cortex from 'within' producing porosity and upon the endocortical surface eroding it 'outwards' enlarging the medullary cavity, (ii) mean tissue mineralization density of the surrounding compact-appearing cortical bone matrix was reduced, (iii) there was a left shift of the void-matrix mineralization density distribution curve relative to controls due to a increased cortical porosity which reducedcortical vBMD. (iv) Mean trabecular vBMD was reduced. (v) Patients with surgically corrected PHPT had

residual but somewhat less severe deficits in several traits.The results were similarat the distal radius but attenuated.

4.1 Cortical deficits

These results, and those using peripheral quantitative computed tomography [14, 15] and high resolution pQCT[16], suggest that endogenous PTH excess results in structural deterioration of both cortical and trabecular bone and that these deficits may be partly reversible [17]. Patients with PHPT had reduced cortical bone area for two reasons. Firstly, intracortical remodeling removed more bone than it replaced leaving void (porosity). Secondly, endocortical resorption eroded the cortex enlarging the medullary area. While endocortical resorption is commonly regarded as a main mechanism responsible for cortical thinning in PHPT and in ageing, the main mechanism we propose that is responsible is intracortical remodeling which thins the cortex from the 'inside' by cavitating the inner compact cortex [4]. The transitional zone area increases at the price of compact appearing cortex as a result of intense remodeling in this region.

During remodelingin advancing age, ~95% of the bone removed by each BMU is replacedwith new bone in these patients. This newly deposited (younger) bone matrix has a lower tissue mineralization density than the bone matrix removed so that there is a left shift in the tissue mineralization density distribution as more void is produced and an increasing proportion of the newly formed osteons have a lower tissue mineral density. Nevertheless, as primary mineralization occurs rapidly and achieves >80% of full mineralization of collagen, little of the deficit in cortical vBMD was due to reduced tissue mineralization density of the newly deposited bone; most of the deficit in cortical vBMDwas the result of increased intracortical porosity produced by the negative BMU balance.

4.2 Trabecular deficits

Intracortical remodeling in the inner cortex produces cortical remnants which resemble true trabeculae (i.e., of growth plate origin). These remnants are erroneously called 'trabeculae' are usually included in quantification of trabecular vBMD. Most imaging methods are not able to distinguish cortical remnants from true trabeculae and therefore show increased or normal trabecular bone volume in PHPT. When these cortical remnants were excluded from the analysis, trabecular vBMD was reduced due primarily to an increase in trabecular separation as the negative BMU balance and high remodeling intensity completely perforate and remove complete plates.

In untreated subjects, trabecular density was reduced while trabecular number and thickness were not reduced. Trabecular density was measured using StrAx1.0 which recognizes the transitional zone and confines assessment of trabecular density to the medullary compartment [13]. Analysis of the trabecular number and thickness was done using the Scanco method [12], which does not recognize the transitional zone and so does not account for cortical trabecularizationwhich erroneously increases trabecular number and likely increases trabecular thickness (as remnants of the cortex may be thick and contain osteons).

Finding that 'trabecular' number was lower in the successfully surgically treated patients is consistent with the notion that reversal of porosity in the inner cortex, which re-corticalizes the fragments (regarded as trabeculae), reduces what is mistakenly called 'trabecular' bone. Evidence of this will require prospective studies. The lack of differences between untreated and successfully surgically treated subjects may reflect the lack of power and that some deficits are irreversible following successful surgery.

4.3 Increased bone remodeling intensity causes bone deficits

Increased bone formation rate determined using dynamic histomorphometry is reported in PHPT[3-10, 13, 18-20]. This measurement is the product of the surface extent of bone formation (reflecting activation frequency or the intensity of bone remodeling) and the mineral apposition rate (MAR).Remodeling intensity and the degree of negativity of the BMU balance vary from surface to surface, but there is no evidence that remodeling events produce a net positive balance upon trabecular surfaces (resulting in trabecular bone gain) and a net negative balance upon the endocortical and intracortical surfaces (resulting in cortical bone loss). The increased in bone forming surfaces upon trabeculae in PHPT is the result of high surface extent of remodeling – there are more BMUs per unit surface area. This will not preserve trabecular bone volume unless the negative BMU balance is corrected. It will not increase trabecular bone volume unless the volume of bone deposited is greater than the volume removed by each of the increased numbers of BMUs. Evidence of increased mean wall thickness or MAR is not compelling. Thus, there is little convincing evidence to support the notion that PTH preserves or increases trabecular bone volume.

4.4 Residual bone deficits post-parathyroidectomy

In many of the parameters measured in the post-parathyroidectomy group, deficits were still present but less so than in untreated patients. The residual deficits suggest that the effects of PTH excess in PHPT are not entirely reversible because the negative BMU balance irreversibly removes complete trabeculae that cannot be reconstructed and produces large coalescent pores that cannot be refilled during the bone formation phase of bone remodeling because of the negative bone balance.

A cautionary note is needed because this was not a prospective study and preoperative morphology was not known. The extent to which these changes can be shown to be reversible

will require prospective studies with long follow-up after parathyroidectomy. Another limitation is that all the controls were recruited in Melbourne, however there were no detectable differences between the Melbourne and New York cases.

5.0 Conclusion

In conclusion, contrary to prevailing notions, PTH excess in PHPT is deleterious both to cortical and trabecular compartments of bone. The normal or high trabecular density reported in several studies is likely to be the result of inclusion of cortical remnants in the medullary compartment. It is likely that these cortical remnants do not function as competent trabecular elements. Data on increased fracture risk in PHPT, albeit limited, may be explained by these observations.

Acknowledgement

The authors wish to thank Ms Karey Cheong for her assistance. Some of this work was supported, in part, by NIH grant DK32333.

References

[1] Hattner R, Epker BN, Frost HM. Suggested sequential mode of control of changes in cell behaviour in adult bone remodelling. Nature 1965;206:489-90.

[2] Seeman E, Delmas PD. Bone quality--the material and structural basis of bone strength and fragility. N Engl J Med 2006;354:2250-61.

[3] Parfitt AM. The physiological and clinical significance of bone histomorphometric data. In: Recker RR, editor. Bone histomorphometry: techniques and interpretation. Boca Raton, FL: CRC Press; 1983. p. 224.

[4] Zebaze RM, Ghasem-Zadeh A, Bohte A, Iuliano-Burns S, Mirams M, Price RI, et al. Intracortical remodelling and porosity in the distal radius and post-mortem femurs of women: a cross-sectional study. Lancet 2010;375:1729-36.

[5] Silverberg SJ, Shane E, de la Cruz L, Dempster DW, Feldman F, Seldin D, et al. Skeletal disease in primary hyperparathyroidism. J Bone Miner Res 1989;4:283-91.

[6] Bilezikian JP. Bone strength in primary hyperparathyroidism. Osteoporos Int 2003;14 Suppl 5:S113-5; discussion S5-7.

[7] Silverberg SJ, Bilezikian JP. Primary hyperparathyroidism. In: DeGroot LJ, Jameson JL, editors. Endocrinology, Sixth Edition. Philadelphia, PA: Elsevier-Saunders; 2010. p. 1176-97.

[8] Parisien M, Silverberg SJ, Shane E, Dempster DW, Bilezikian JP. Bone disease in primary hyperparathyroidism. Endocrinol Metab Clin North Am 1990;19:19-34.

[9] Dempster DW, Parisien M, Silverberg SJ, Liang XG, Schnitzer M, Shen V, et al. On the mechanism of cancellous bone preservation in postmenopausal women with mild primary hyperparathyroidism. J Clin Endocrinol Metab 1999;84:1562-6.

[10] Dempster DW, Muller R, Zhou H, Kohler T, Shane E, Parisien M, et al. Preserved three-dimensional cancellous bone structure in mild primary hyperparathyroidism. Bone 2007;41:19-24.

[11] Han ZH, Palnitkar S, Rao DS, Nelson D, Parfitt AM. Effect of ethnicity and age or menopause on the structure and geometry of iliac bone. J Bone Miner Res 1996;11:1967-75.

[12] Laib A, Hauselmann HJ, Ruegsegger P. In vivo high resolution 3D-QCT of the human forearm. Technol Health Care 1998;6:329-37.

[13] Zebaze R, GhasemZadeh A, Mbala A, Seeman E. A New Method of Segmentation of Compact-Appearing, Transitional and Trabecular Compartments and Quantification of Cortical Porosity from High Resolution Peripheral Quantitative Computed Tomographic Images. Bone 2013;54:8-20

[14] Charopoulos I, Tournis S, Trovas G, Raptou P, Kaldrymides P, Skarandavos G, et al. Effect of primary hyperparathyroidism on volumetric bone mineral density and bone geometry assessed by peripheral quantitative computed tomography in postmenopausal women. J Clin Endocrinol Metab 2006;91:1748-53.

[15] Chen Q, Kaji H, Iu MF, Nomura R, Sowa H, Yamauchi M, et al. Effects of an excess and a deficiency of endogenous parathyroid hormone on volumetric bone mineral density and bone geometry determined by peripheral quantitative computed tomography in female subjects. J Clin Endocrinol Metab 2003;88:4655-8.

[16] Hansen S, Beck Jensen JE, Rasmussen L, Hauge EM, Brixen K. Effects on bone geometry, density, and microarchitecture in the distal radius but not the tibia in women with primary hyperparathyroidism: A case-control study using HR-pQCT. J Bone Miner Res 2010;25:1941-7.

[17] Hansen S, Hauge EM, Rasmussen L, Jensen JE, Brixen K. Parathyroidectomy improves bone geometry and microarchitecture in female patients with primary hyperparathyroidism: a one-year prospective controlled study using high-resolution peripheral quantitative computed tomography. J Bone Miner Res 2012;27:1150-8.

[18] Parisien M, Cosman F, Mellish RW, Schnitzer M, Nieves J, Silverberg SJ, et al. Bone structure in postmenopausal hyperparathyroid, osteoporotic, and normal women. J Bone Miner Res 1995;10:1393-9.

[19] van Doorn L, Lips P, Netelenbos JC, Hackeng WH. Bone histomorphometry and serum concentrations of intact parathyroid hormone (PTH(1-84)) in patients with primary hyperparathyroidism. Bone Miner 1993;23:233-42.

[20] Delling G. Bone morphology in primary hyperparathyroidism--a qualitative and quantitative study of 391 cases. Appl Pathol 1987;5:147-59.

Figure Legends

Figure 1. Segmentation and quantification of HR-pQCT images by StAx1.0.(A) The acquired grey scale image. (B and C) StrAx1.0 segments bone from the soft tissue background, and segments bone into its compact-appearing cortical, outer and inner transitional zones, and the trabecular compartment. Total cortex comprises compact-appearing cortex, inner transitional zone and outer transitional zone. Color-coding is based on the proportion of mineralized matrix and void volumes in each voxel.

Figure 2. Distal tibia (A, C) and radius (B, D) morphology expressed as Z scores adjusted for height and weight (mean ± SEM). To adjust for bone size, morphology is expressed asthe proportion of the total bone cross-sectional area. Total cortical area, compact-appearing cortical (CC) area, outer transitional zone (OTZ), inner transitional zone (ITZ) and medullary area are shown in patients with untreated primary hyperparathyroidism (PHPT) and surgically treated patients. Cortical morphology with total cortical volumetric bone mineral density (vBMD) determined by total cortical porosity (comprising CC; OTZ, ITZ) and tissue mineralization density (mineralization). *$p<0.05$ compared to zero

Figure 3. Distal tibia (A) and radius (B) trabecular (trab) morphology (vBMD, number, thickness and separation). *$p<0.05$ compared to zero.

Figure 4. Frequency or void-bone matrix distribution curve of voxels within the compact-appearing cortex of the distal tibia (A) and distal radius (B). Voxels on the left contain only void volume (0%), more void than mineralized bone matrix volume, more mineralised bone matrix than void volumes, and only mineralized bone matrix volume on the right (100%). Relative to controls, untreated PHPT had a left shift. Relative to untreated PHPT, treated PHPT had a right shift. These relative shifts were similar in both distal tibia and radius.

Figure 1.

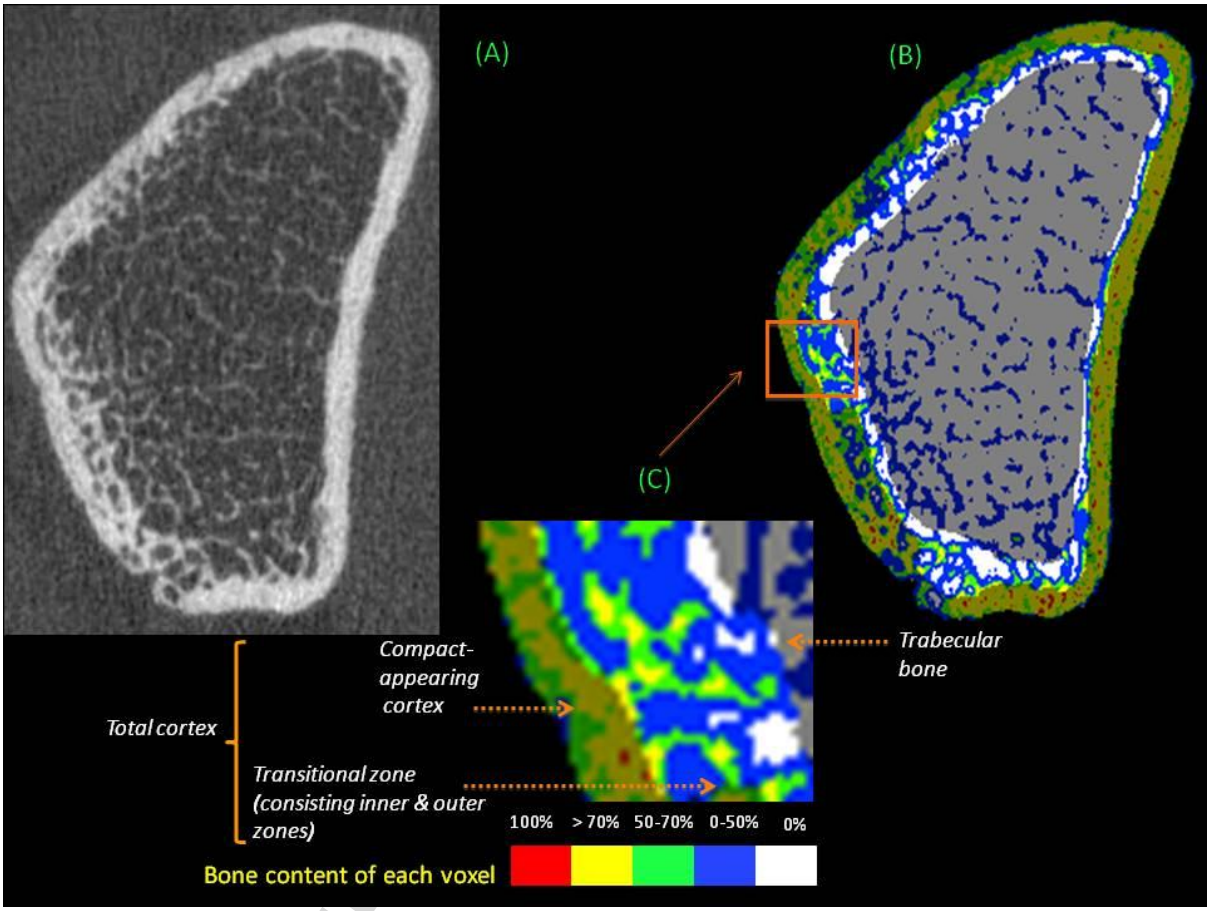

Figure 2.

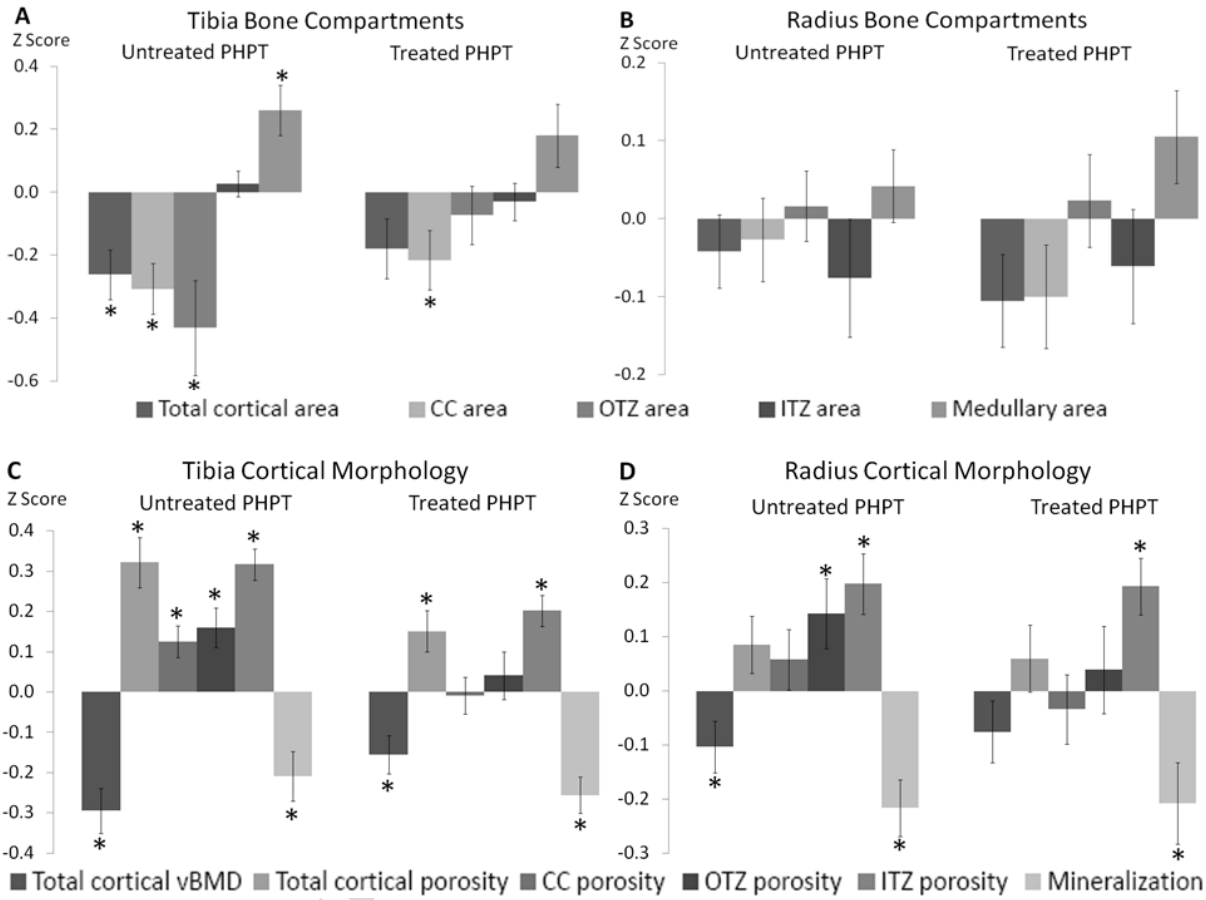

Figure 3.

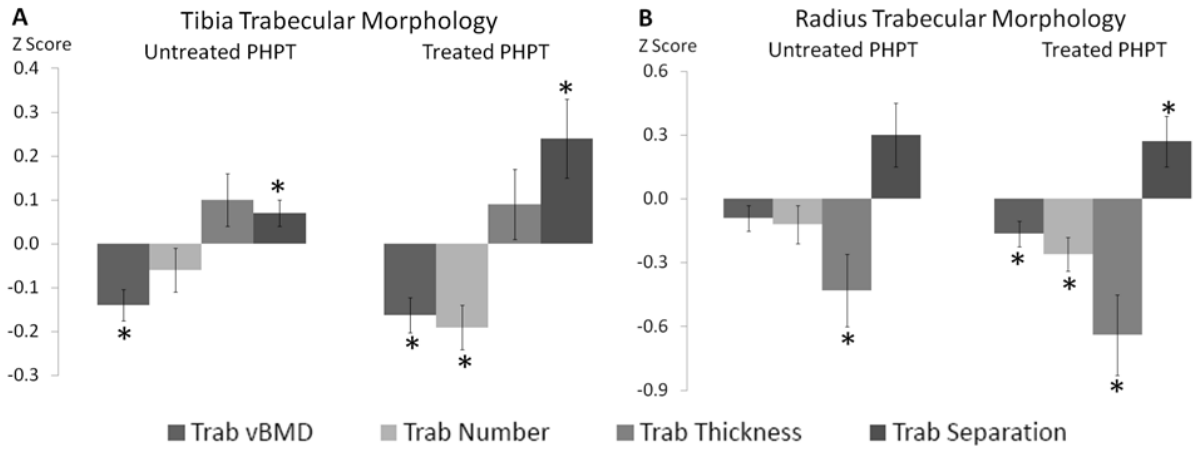

Figure 4.

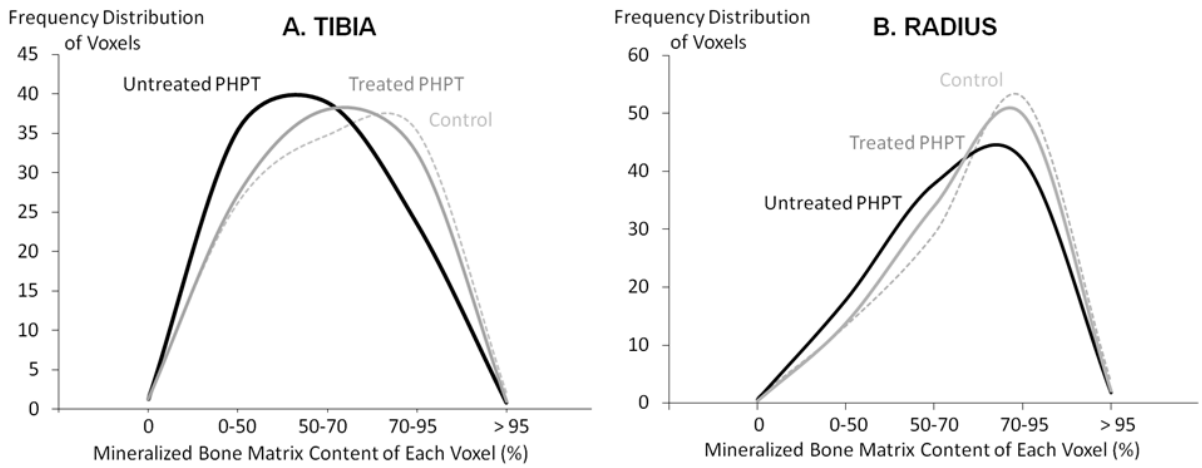

Tables

Table 1. Baseline patient characteristics

	Untreated PHPT (n = 43)	**Treated PHPT** (n = 25)	**Controls** (n = 47)	**Reference ranges**
Age (years)	62.9 ± 13.8	63.6 ± 13.6	61.1 ± 14.9	
Height (m)	1.63 ± 0.11	1.64 ± 0.09	1.66 ± 0.10	
Weight (kg)	78.9 ± 18.0	75.3 ± 16.7	74.4 ± 13.5	
Female:Male	31:12	17:8	31:16	
Caucasian:Hispanic:African American	41:1:1	24:1:0	47:0	
Melbourne:New York patients	31:12	15:10	47:0	
Time since diagnosis (years)	1.9 ± 2.0			
Time since surgery (years)		5.3 ± 5.3		
Corrected serum calcium (mmol/L)	2.66 ± 0.16[ab]	2.41 ± 0.20[a]	2.42 ± 0.11[b]	2.10 – 2.60
Serum phosphate (mmol/L)	1.02 ± 0.21	1.10 ± 0.16	1.24 ± 0.20	0.60 – 1.40
Serum PTH (pmol/L)	13.0 ± 5.7[ab]	6.4 ± 4.3[a]	4.1 ± 0.9[b]	1.6 – 6.9
Serum 25(OH)D (nmol/L)	58.9 ± 13.8	55.4 ± 18.1	54.5 ± 23.3	>75[c]
% supplementated with cholecalciferol	48	47	45	
% supplementated with calcium	0	26	20	

Values expressed as mean ± SD

[a]Untreated PHPT vs. Treated PHPT $p < 0.05$

[b]Untreated PHPT vs. Control $p < 0.05$

[c]Represents the desirable level of 25(OH) vitamin D at our institution

Table 2. Bone morphology expressed as Z scores (mean ± SEM)

	Untreated PHPT		Treated PHPT	
	Tibia	**Radius**	**Tibia**	**Radius**
Bone Compartments				
Total cortical area	-0.26 ± 0.08$^{\beta}$	-0.04 ± 0.05	-0.18 ± 0.10	-0.11 ± 0.06
CC area	-0.31 ± 0.08$^{\gamma}$	-0.03 ± 0.05	-0.22 ± 0.09$^{\alpha}$	-0.10 ± 0.07
OTZ area	-0.43 ± 0.15$^{\beta}$	0.02 ± 0.05	-0.07 ± 0.09	0.02 ± 0.06
ITZ area	0.03 ± 0.04	-0.08 ± 0.08	-0.03 ± 0.06	-0.06 ± 0.07
Medullary area	0.26 ± 0.08$^{\beta}$	0.04 ± 0.05	0.18 ± 0.10	0.11 ± 0.06
Cortical Morphology				
Total cortical vBMD	-0.29 ± 0.06$^{\gamma}$	-0.10 ± 0.05$^{\alpha}$	-0.15 ± 0.05$^{\beta}$	-0.08 ± 0.06
Total cortical porosity	0.32 ± 0.06$^{\gamma}$	0.09 ± 0.05	0.15 ± 0.05$^{\beta}$	0.06 ± 0.06
CC porosity	0.13 ± 0.04$^{\beta}$	0.06 ± 0.06	-0.01 ± 0.05	-0.03 ± 0.06
OTZ porosity	0.16 ± 0.05$^{\beta}$	0.14 ± 0.06$^{\alpha}$	0.04 ± 0.06	0.04 ± 0.08
ITZ porosity	0.32 ± 0.04$^{\gamma}$	0.20 ± 0.06$^{\alpha}$	0.20 ± 0.04$^{\gamma}$	0.19 ± 0.05$^{\alpha}$
Tissue Mineralization Density	-0.21 ± 0.06$^{\beta}$	-0.22 ± 0.05$^{\gamma}$	-0.26 ± 0.04$^{\gamma}$	-0.21 ± 0.08$^{\alpha}$
Trabecular Morphology				
Trabecular vBMD	-0.14 ± 0.04$^{\gamma}$	-0.09 ± 0.06	-0.16 ± 0.04$^{\gamma}$	-0.16 ± 0.06$^{\alpha}$
Trabecular number^	-0.06 ± 0.05	-0.12 ± 0.09	-0.19 ± 0.05$^{\gamma}$	-0.26 ± 0.08$^{\gamma}$
Trabecular thickness^	0.10 ± 0.06	-0.43 ± 0.17$^{\alpha}$	0.09 ± 0.08	-0.64 ± 0.19$^{\gamma}$
Trabecular separation^	0.07 ± 0.03$^{\alpha}$	0.30 ± 0.15	0.24 ± 0.09$^{\alpha}$	0.27 ± 0.12$^{\alpha}$

Area is expressed as a proportion of the total bone cross-sectional area

CC (compact-appearing cortex)

OTZ (outer transitional zone)

ITZ (inner transitional zone)

$^{\alpha}$p value <0.05 compared to zero

$^{\beta}$p value <0.01 compared to zero

$^{\gamma}$p value <0.001 compared to zero

$^{\wedge}$parameter derived from Scanco Medical AG software

Highlights

- Endogenous PTH excess is deleterious to both cortical and trabecular bone
- Cortical bone area was reduced
- Cortical vBMD was reduced due to increased cortical porosity and reduced tissue mineralization density
- Trabecular vBMD was reduced
- Patients with surgically corrected PHPT had residua,l but less severe, deficits in several traits